CHAPTER IV

Exacerbation of the liver fibrosis by retinoid via TGF-β

IV-1. Introduction

HSCs are the major storage sites of vitamin A in normal liver. In liver injury they are the cells responsible for extracellular matrix production by virtue of their ability to undergo "activation" (27, 28). HSC activation refers to their transformation into myofibroblastic cells, during which they lose lipid droplets containing vitamin A (27, 28). Major unresolved issues about the role of vitamin A (retinol) and its derivatives (retinoids) in liver fibrosis have been the mechanisms of intracellular retinoid loss and the potential roles this loss may play in facilitating cellular activation and hepatic fibrosis.

In the previous chapters, I described that retinoid up-regulates the expression of uPA and other related genes in the vascular endothelial cells through physical interaction between RAR/RXR and Sp1, resulting in TGF-β-mediated suppression of embryonic angiogenesis. TGF-β accelerates HSC activation; it stimulates HSCs to transform into myofibroblast-like cells, enhances their production of extracellular matrix proteins (2, 87-89), and alters the degradation of the extracellular matrix (87, 90). Furthermore, TGF-β suppresses the growth and function of hepatocytes, at least in part, by down-regulating the production of hepatocyte growth factor.

Taken together, these findings suggest that retinoids might induce the formation of TGF-β in liver HSCs, thereby exacerbating the progression of fibrogenesis. In the present study, I disclose the formation of a novel stereoisomer of RA during the hepatic fibrosis and examined above hypothesis using an *in vitro* model of rat HSC cultures, as well as an *in vivo* model of porcine serum-induced hepatic fibrosis in rats.

IV-2. Materials and Methods

Materials

All-*trans*-retinol, atRA, and 13cRA were purchased from Sigma (St. Louis, MO). 9cRA and 9,13dcRA were obtained from Wako Pure Chemical Industries Ltd. (Osaka, Japan). Monoclonal anti-TGF-β antibody, which neutralizes TGF-β1, -β2, and - β3, was obtained from Genzyme Diagnostics.

Induction of liver fibrosis in rats

Male Wistar rats (100~120 g body weight; Nihon Charles-River, Atsugi, Japan) were allowed free access to standard chow pellets (Oriental Yeast Co., Tokyo, Japan) and distilled water throughout the experiments. Liver fibrosis was induced in 6 rats by repeated intraperitoneal injections of 0.5 ml of porcine serum twice a week for up to 12 weeks. The same number of rats received repeated intraperitoneal injections of saline and served as controls. Twelve weeks later, both the porcine serum-treated and control rats were sacrificed, the livers were perfused with PBS and excised. Half of each liver was quickly frozen in liquid nitrogen and stored at -80°C until the chemical analyses were performed, and the other half was fixed in 10% buffered formalin solution for 24 h at room temperature for histologic analysis.

Design of the animal experiments to assess exogenously administrated retinoid

Liver fibrosis was induced in 20 rats by repeated intraperitoneal injections of 0.5 ml of porcine serum twice a week for up to 12 weeks. Half of these porcine serum-treated rats as well as 10 normal rats were received the acyclic retinoid mixed with peanut oil via a stomach tube, at a dose of

40 mg per kg of body weight 5 times a week from the beginning of the administration of the porcine serum. This synthetic retinoid exerts comparable activity to atRA with less cytotoxicity (91) through direct activation of RARs (92). The acyclic retinoid dose that I employed caused neither significant loss of body weights nor decline of food intakes. The other 10 porcine serum-treated rats as well as 10 normal rats were received only peanut oil as a placebo. Eight and 12 weeks later, 5 rats in each group were anesthetized by the intravenous injection of sodium pentobarbital, killed, and bled from the abdominal aorta. The livers were perfused with PBS, dissected out, frozen in liquid nitrogen, and stored at -80°C until the determination of hydroxyproline content. The same experiment was repeated for the histologic study and TGF-β determination of the liver, with an exception that all 40 rats (10 each × 4 groups) were killed after 12 weeks. Half portion of the livers was fixed in 10% buffered formalin solution for 24 h at room temperature, to prepare sections for histologic analyses. Another half of the livers was subjected to the measurement of TGF-β concentrations.

Extraction of RAs and HPLC analysis

The extraction and analysis of RA isomers with high-performance liquid chromatography (HPLC) were performed as previously described (93). The extraction of RA from HSC cultures and the liver was carried out quickly in opaque test tubes under nitrogen gas with special cares to minimize *in vitro* oxidization (93). The HPLC system consisted of two LC-10AS pumps, a SPD-10 UV/VIS spectrophotometric detector, a SLC-10A system controller, a C-R6A integrator, and a CTO-10A column oven (Shimadzu Co., Kyoto, Japan). RA isomers were assessed by reverse-phase HPLC with Wakoshil II 5-C18-AR column (0.46 x 30 cm, Wako Pure Chemical Industries;

Refs. 94, 95) taking synthetic RA isomers as the internal standards (93).

Assay of transactivation activity

HeLa cells were maintained in phenol red-free Dulbecco's modified Eagle medium (DMEM; Gibco) containing 5% dextran-coated, charcoal-stripped fetal calf serum. The cells were transfected at 40-50% confluence in 9 cm Petri dishes using calcium phosphate precipitation. Either a combination of 1 μg of reporter plasmid, 17m2-Globin-CAT, and 0.5 μg of the expression vector, GAL4-RARα (DEF) or GAL4-RXRα (DE) (50), or a combination of 1 μg of the reporter plasmid, DR5-Globin-CAT, with 0.5 μg each of the expression vectors for RARα and RXRα, was co-transfected in the presence of 3 μg of a β-galactosidase expression vector, pCH110 (Pharmacia), serving as internal control to normalize variations in transfection efficiency. Bluescribe M13+ (Stratagene) was used as a carrier to adjust the total amount of DNA to 20 μg. After a 20 h-incubation with the DNA, the cells were washed with fresh medium and incubated for an additional 12 h. The cells were incubated for another 12 h with various concentrations of 9,13dcRA. Thereafter, cell extracts were prepared and subjected for CAT assays after normalizing β-galactosidase activity (50).

Zymography

Zymography was carried out as described previously (13). After proteins in the culture medium were separated by SDS-polyacrylamide gel electrophoresis, the gels were washed with 2.5% Triton X-100 and with PBS, applied onto fibrin-agar containing plasminogen, and incubated at 37°C until uPA- or tPA-derived lysis band were detected.

Preparation of acid-ethanol extracts of liver tissues

Tissue extracts for the TGF-β assays were prepared according to the method of Khalil et al (96). Briefly, a portion of each rat liver (approximately 1 g each) was disrupted in 95% ethanol-0.2 M HCl solution at 4°C for 36 h. The resulting homogenates were centrifuged at 10,000 x g for 10 min, and the supernatants were lyophilized. The tissue extracts were reconstituted in 1 ml of 4 mM HCl containing 0.1% BSA, sonicated, and filter-sterilized. Tissue extracts for protein assays were prepared simultaneously by homogenizing another piece of the same liver in 50 mM imidazole buffer, pH 7.4 containing 0.8% NaCl and 1.0% Triton X-100, followed by centrifugation at 10,000 x g for 10 min after adding the Cell Debris Remover (Sigma). Both extracts were kept at -80°C until the assays for either TGF-β or protein contents. The acid-ethanol extracts were neutralized prior to the measurement of their TGF-β concentration.

Assay of TGF-β concentration

Active TGF-β was assayed by the inhibition of [^{3}H]thymidine incorporation by CCL-64 mink lung epithelial cells, as described previously (23). The amount of TGF-β in the conditioned medium as well as in various extracts was determined by comparison to a standard curve made with rTGF-β 1. The amount of total (latent plus active) TGF-β in the sample was determined in a similar manner after all the latent TGF-β in the sample had been converted to active TGF-β by acidification of the sample (pH 3; 1 h at room temperature), followed by neutralization. Data are expressed as the amount of TGF-β secreted from 10^5 cells. For example, if the concentration of TGF-β in 0.5 ml of culture medium, collected from confluent cultures of 1.5 x 10^5 HSCs, was 3 pM (75 pg/ml), this would be expressed as 1 fmol/10^5 cells. The amount of total TGF-β in ethanol-

acid extracts of liver tissues was expressed as pmol TGF-β per mg protein. The protein concentration was measured by BCA (Pierce) assays, using BSA as the standard. The specificity of the inhibition of the [^{3}H]thymidine incorporation was validated by controls employing anti-TGF-β antibodies added to the sample. Since RA itself had a little effect on the [^{3}H]thymidine incorporation, every sample was irradiated under UV light to destroy RA prior to the assay. The present bioassay can be used to measure TGF-β in the range of 0.08-2.4 pM (23). I determined the TGF-β concentration of each sample by measuring the concentration in eight serial dilutions.

Assay of collagen synthesis in HSCs

The human HSC line, LI90, was kindly supplied by Dr. K. Murakami (Tohoku University, Sendai, Japan) and maintained in DMEM containing 10% fetal calf serum. LI90 cells used in the present study represented the activated HSCs or myofibroblast-like phenotype. Details of characterization of this cell line have been described in the previous paper (97). Isolation and primary culture of rat HSCs were carried out according to the method of Kawada et al. (98). Preparation of cell lysates for Northern analysis was performed as described in the chapter I. The amount of collagen synthesized was determined as described previously (99). Briefly, after HSC cultures were incubated with 9,13dcRA, cultures were pre-incubated for 30 min with 100 μM ascorbic acid and 500 μM aminopropionitrile, and labeled with 1 μM (100 μCi/ml) [^{3}H]proline (Amersham) for 3 h. Thereafter, cell lysates were prepared in 50 mM Tris buffer, pH 7.4 containing 0.5% Triton X-100 and 10 μg/ml each of four different types of collagen as the unlabeled carrier. Proteins in the lysate were separated by SDS-5% polyacrylamide gel electrophoresis. The gels were dried following the staining and fluorography was performed. Type I collagen was

identified as the radioactive band that migrated to the same position as the carrier collagen, and was quantitated by densitometry as described previously (13).

Measurement of tissue hydroxyproline content

The tissue levels of hydroxyproline were determined as described previously (100).

Histology

Portions of livers fixed in 10% buffered formalin solution were dehydrated in ethanol and embedded with paraffin. Sections (2 μm thick) were stained by Azan-Mallory method. Liver fibrosis was graded from stage 0 to III, according to the criteria used in the numerical scoring system proposed by Knodell et al (101), regardless of the treatment and the results of the chemical analyses. Grade 0 represented no fibrosis; grade I represented slight fibrosis with fibrous portal expansion; grade II, moderate fibrosis with portal-portal or portal-central linkages; and grade III, severe fibrosis accompanied by cirrhosis, in which loss of the normal hepatic lobular architecture, with fibrous septa separating and surrounding nodules was observed.

Statistics

Statistics were calculated by Mann-Whitney-Wilcoxon test for Table IV-1 and by Dunnett's *t*-test for others.

IV-3. Results

9,13dcRA levels are increased in in vivo *fibrotic liver and in activated HSCs*

To know whether hepatic stored retinol is metabolized during the progression of liver fibrosis, I determined the composition of hepatic retinoids following induction of fibrosis in rat livers by continuous administration of porcine serum for 12 weeks (Fig. IV-1A). Retinol content was decreased by 66% in agreement with analyses in human and experimental liver disease (27, 28). Instead, there were approximately 58% increases in atRA and 114% increase in 9,13dcRA, a recently described novel species of RA stereoisomer (102, 103), in fibrotic liver. Neither 9cRA nor 13cRA was detectable. Similar changes except those in 13cRA were observed during activation of rat primary HSCs *in vitro* (Fig. IV-1B). Following 7 days culture on plastic dish, retinol content in the cells was decreased by 80%, as described previously (27, 28), and, instead, there were, respectively, 33%, 33%, and 60% increases in atRA, 13cRA, and 9,13dcRA, compared to the cells cultured for 1 day. 9cRA was not detectable. Next, to know if this novel stereoisomer of atRA has biological activities, I assessed its activity to transactivate RARα by reporter assays. As HSCs were likely to contain high levels of endogenous RAs, I used HeLa cells which had been maintained in retinoid-depleted condition. As depicted in Fig. IV-2, 9,13dcRA activated RARα-dependent Gal4-fusion transactivator (*panels A*) as well as RARα/RXRα heterodimer (*panel C*), but did not activate RXRα-dependent Gal4-fusion transactivator at all (*panel B*).

Effect of 9,13dcRA on HSC culture

I next explored the hypothesis that 9,13dcRA may play a role in the progression of the liver fibrosis via stimulating the production of TGF-β and its proteolytic activation initiating from the

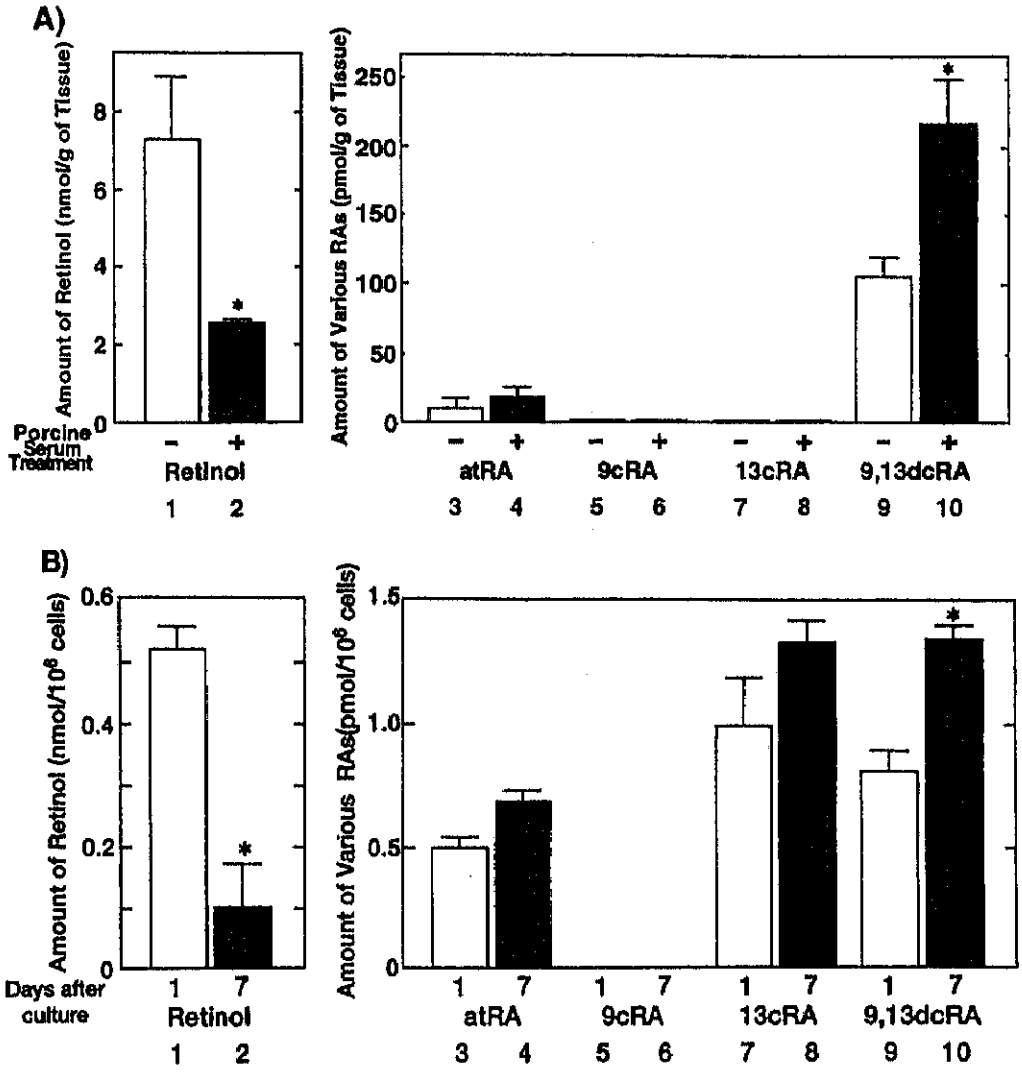

Fig. IV-1. Increase in 9,13dcRA levels in the fibrotic liver and activated HSCs. A) Liver fibrosis was induced in 6 rats by continuous intraperitoneal injections of porcine serum for 12 weeks. Animals were sacrificed, livers were isolated, and retinoids were extracted. The concentration of retinol (columns 1 and 2), atRA (columns 3 and 4), 9cRA (columns 5 and 6), 13cRA (columns 7 and 8), and 9,13dcRA (columns 9 and 10) were determined by HPLC analyses and expressed as either nanomoles or picomoles of each retinoid per gram of liver weight. Odd numbers: control rats administered saline; even numbers: fibrotic rats administered porcine serum. Each value represents the average ± SD (n=6). Asterisks represent significant differences ($p<0.05$) obtained by a comparison between control and porcine serum-treated rats. The experiment was repeated twice. B) Retinoids were extracted from primary rat HSCs cultured for either 1 day or 7 days on plastic dishes in DMEM containing 10% fetal calf serum. Concentration of each retinoid was determined by HPLC as described above and expressed as either nanomoles or picomoles of each retinoid per 10^6 cells. Odd numbers: HSCs cultured for 1 day; even numbers: HSCs cultured for 7 days. Each value represents the average ± SD (n=5). Asterisks represent significant differences ($p<0.05$) obtained by a comparison between 1 day and 7 days. The experiment was repeated three times.

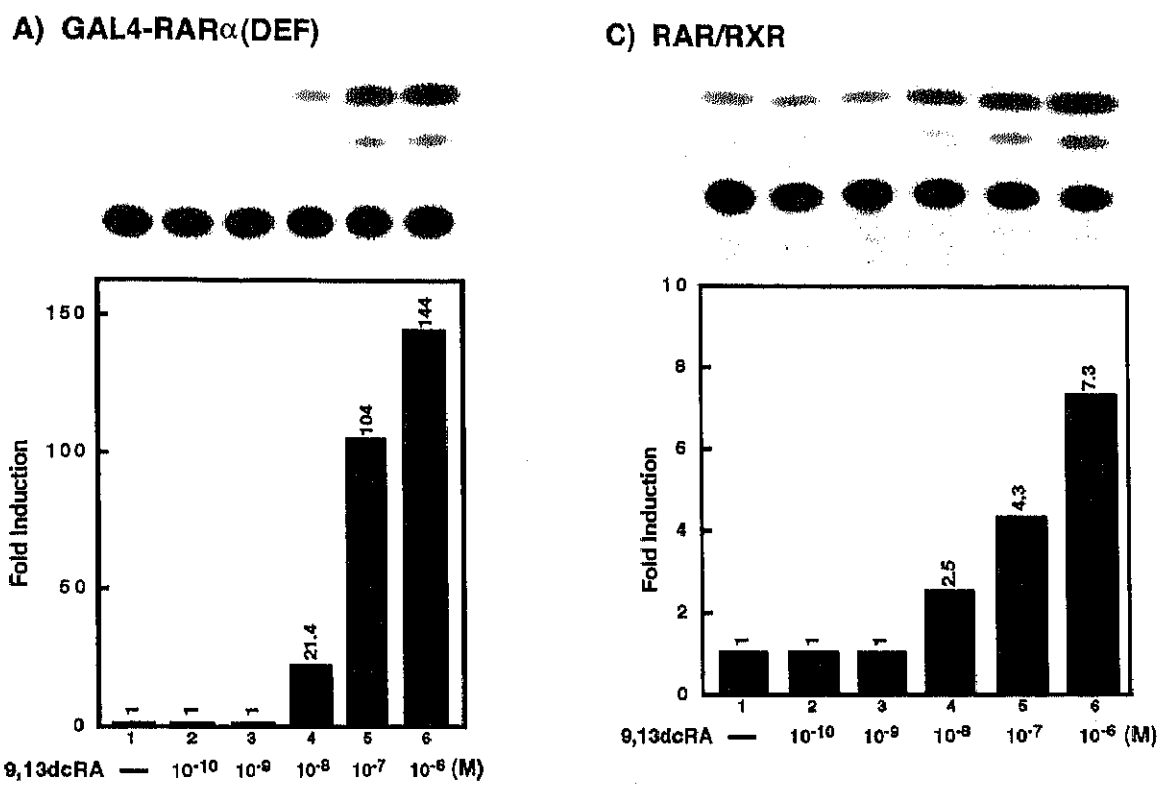

Fig. IV-2. Transactivation activity of 9,13dcRA. HeLa cells were co-transfected with combination of the reporter plasmid, 17m2-Globin-CAT and expression vector, GAL4-RARα (DEF) (panel A), combination of 17m2-Globin-CAT and GAL4-RXRα (DE) (panel B), or combination of the reporter plasmid, DR5-Globin-CAT and both of the expression vectors for RARα and RXRα (panel C). Cells were then treated with the indicated concentrations of 9,13dcRA for 12 h as described in the Materials and Methods. Cell extracts were prepared and CAT activity in each extract was measured. Densitometric analysis was performed and the results are presented by both bar graph and relative fold induction written above each bar. Each experiment was repeated four times, and representative results are shown.

activation of RARα. I examined the biological activity of 9,13dcRA toward HSCs. I first compared the amount of PA present in the culture medium derived from two different kinds of HSCs, between untreated cells and 9,13dcRA-treated cells (Fig. IV-3). Rat primary HSCs produced and secreted predominantly uPA (*lane 1*), whereas human SC cell line, LI90 cells, produced and secreted tPA as a dominant species (*lane 3*). 9,13dcRA enhanced both uPA levels in rat primary HSCs and tPA levels in human LI90 cells (*lanes 2* and *4*, respectively). uPA has a highly strict species specificity and there is no cross-reactivity between probes derived from different species. In contrast, tPA does not have such a species specificity. Because I could not obtain a probe for rat uPA, I decided to analyze the mechanism of 9,13dcRA-induced tPA expression and potential formation of TGF-β by LI90 cells. As seen in Fig. IV-4, 9,13dcRA enhanced both cellular PA/plasmin (*panel A*) and TGF-β (*panel B*) levels in LI90 cell cultures, and the induction of TGF-β was suggested to be dependent upon plasmin since an inhibitor of plasmin, aprotinin, alleviated 9,13dcRA-induced formation of TGF-β (*panel B*, *lane 3*), as in the case in endothelial cells (23). This suggests that 9,13dcRA-treatment elaborated proteolytic activation of latent TGF-β in human HSCs via up-regulation of tPA production. Because I treated LI90 cells in the serum-free medium after rinsing the cultures with PBS, the source of surface plasmin is thought to be serum plasminogen bound to the cell surface during subculture (101). Figure IV-5 shows the result of changes induced in the mRNA levels of several related genes following the exposure of LI90 cells to 9,13dcRA. Untreated LI90 cells expressed nominal levels of RARβ and RARγ, but very low level of RARα. Upon treatment with 9,13dcRA, the expression of RARα and tPA increased simultaneously, suggesting the possible involvement of RARα in the up-regulation of tPA

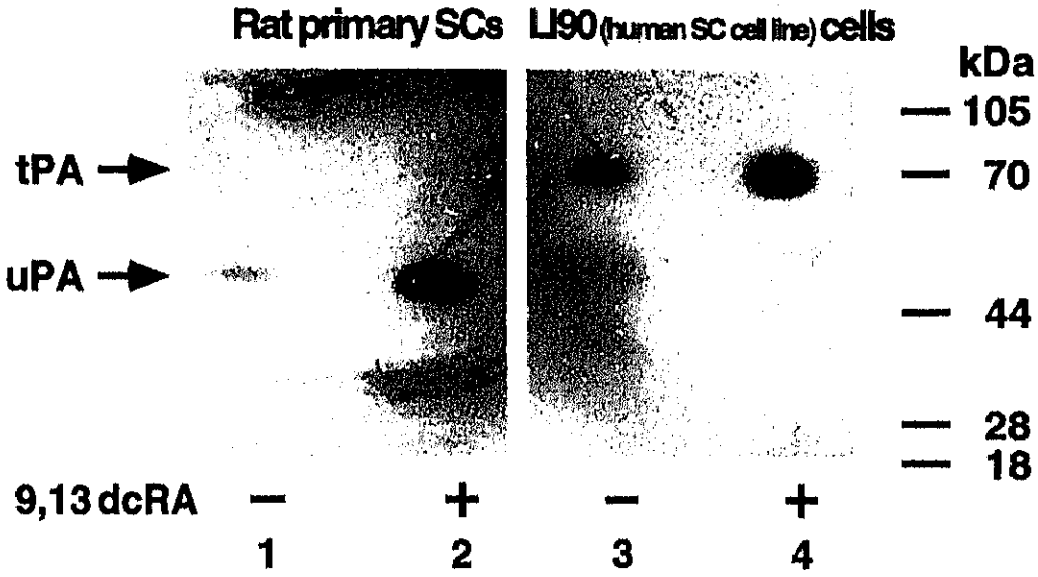

Fig. IV-3. Augmentation of uPA secretion from the rat primary HSC cultures and tPA secretion from the cultures of human SC line, LI90 by 9,13dcRA. Confluent rat primary SCs or LI90 cells were incubated either with vehicle (control) or with 1 μM 9,13dcRA in serum-free DMEM for 12 h. The conditioned medium was collected, concentrated 100-fold on Microcon concentrator (Amicon) and subjected to SDS-PAGE with a 10% resolving gel. The gel was washed, applied onto fibrin-agar gel containing plasminogen and incubated until uPA- or tPA-derived lysis bands were detected. Lane 1, control rat SCs; lane 2, 9,13dcRA-treated rat SCs; lane 3, control LI90 cells; lane 4, 9,13dcRA-treated LI90 cells.

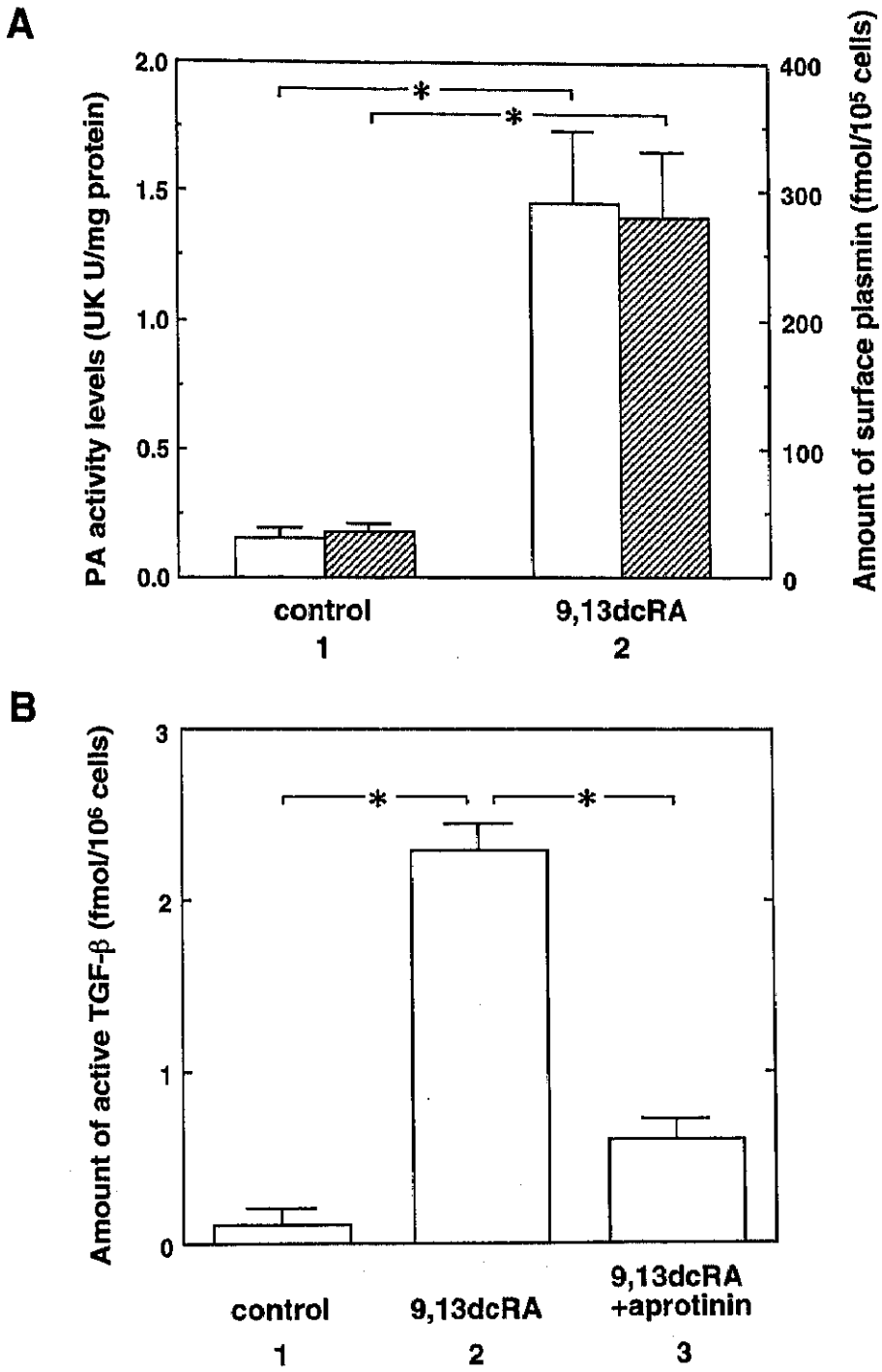

Fig. IV-4. Enhancement of HSC PA/plasmin and TGF-β levels by 9,13dcRA. A) After treatment of LI90 cells with 1 μM 9,13dcRA for 12 h in DMEM-BSA, either cellular PA (open column) or surface plasmin (slashed column) was recovered from the cultures and both activity levels were determined. B) The culture medium was collected and the levels of active TGF-β in the medium were measured as described in the Materials and methods. Sample 1, control cells; sample 2, 9,13dcRA-treated cells; sample 3, 9,13dcRA-treated cells in the presence of 50 μg/ml aprotinin. *: $P<0.01$.

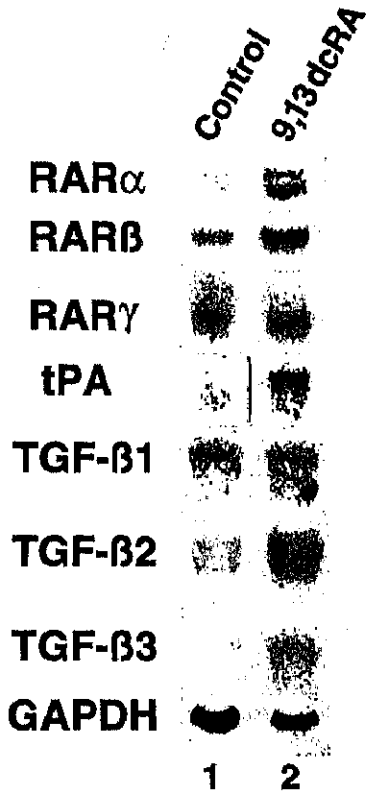

Fig. IV-5. Changes in the mRNA levels of RARα, β, γ, tPA and TGF-β1, -β2, -β3 following the exposure of LI90 cells to 9,13dcRA. Confluent LI90 cell cultures were incubated either with vehicle (control; lane 1) or with 1 μM 9,13dcRA (lane 2) in DMEM-BSA for 12 h. Total RNA was isolated from each cell sample, fractionated through 1% agarose-formaldehyde gels, transferred onto nylon membranes and hybridized with ^{32}P-labeled probe for RARα, β, γ, tPA, TGF-β1, -β2, -β3 or GAPDH. The radioactivity of each band was detected on an imaging analyzer.

expression, similar to what I have seen in BAECs in the chapter I. The expression of RARβ was also enhanced by 9,13dcRA, but the expression of RARγ was minimally affected. TGF-β2 and -β3 expressions were also increased by 9,13dcRA-treatment, supporting the potential linkage between the enhanced tPA production and the induction of TGF-β in LI90 cells.

Next, in order to test whether RARα played an important role in 9,13dcRA-induced tPA expression and subsequent TGF-β formation by LI90 cells, I examined the effects of RAR-subtype specific agonists as well as antagonists. Figure IV-6 shows the result of agonists. LI90 cells were treated with various concentrations of 9,13dcRA or each RAR subtype-selective retinoid, and both cellular PA activity and active TGF-β levels in the medium were measured. Among retinoids tested, 9,13dcRA, pan-RAR-selective Ch55 and RARα-selective Am580 enhanced both PA (*panels a-c*, respectively) and TGF-β (*panels f-h*, respectively) levels. I can not explain why, roughly estimated, about 10 times higher concentrations of these retinoids were required for induction of TGF-β compared with those required for enhancement of PA levels. In contrast, no induction was observed in both PA and TGF-β levels with RARβ -selective retinoid (CD2019; *panels d* and *i*) or RARγ-selective retinoid (CD437; *panels e* and *j*). These results suggest that activation of RARα may mediate 9,13dcRA-induced tPA production and thus TGF-β formation. This was confirmed by testing the effect of subtype specific antagonist (Fig. IV-7). Both 9,13dcRA- and Ch55-induced up-regulations were blocked significantly by the co-addition with RARα-selective antagonist, Ro41-5253, and weakly with RARβ-selective antagonist, LE135. The PA and TGF-β levels were decreased by approximately 60~70% with Ro41-5253 and by approximately 25~30% with LE135. Collectively, it is suggested that 9,13dcRA may enhance tPA production and thereby induce the activation of latent TGF-β in LI90 cells, at least in part (~60%) through the induction and

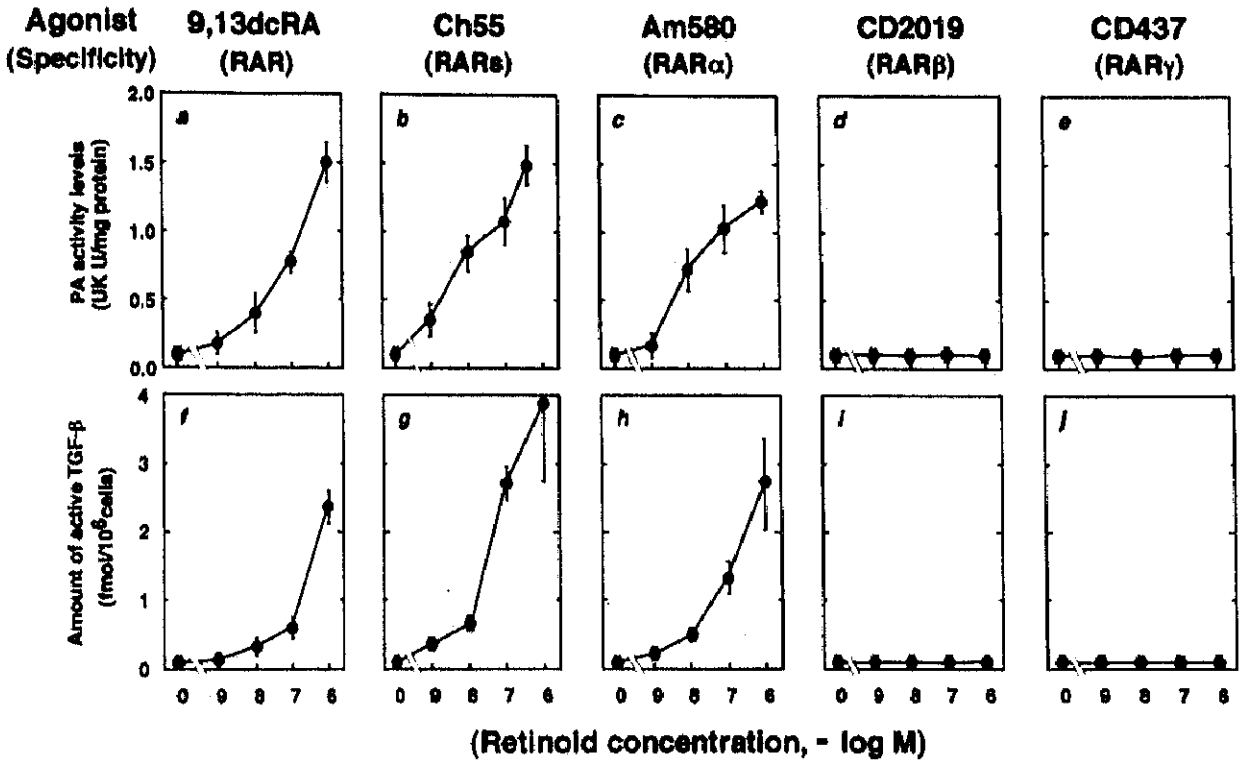

Fig. IV-6. Enhancement of cellular PA levels and induction of TGF-β formation by RARα-selective retinoid in LI90 cell cultures. After confluent LI90 cell cultures were incubated in DMEM-BSA for 12 h with various concentrations of 9,13dcRA or each subtype-specific retinoid, cellular PA activities (panels a-e) and active TGF-β levels in the medium (panels f-j) were measured as before.

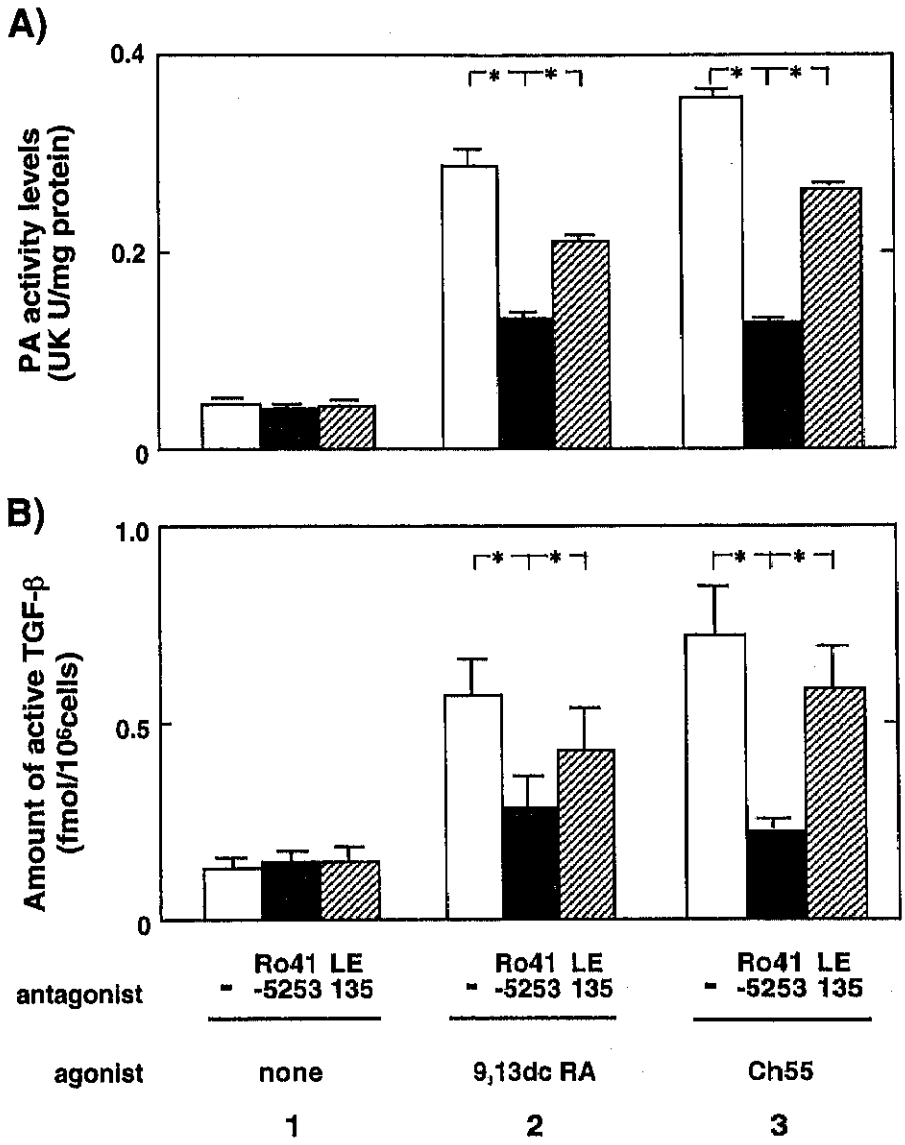

Fig. IV-7. Effect of subtype-selective retinoid antagonists on the induction by 9,13dcRA of cellular PA and active TGF-β in LI90 cells. Confluent LI90 cell cultures were incubated in DMEM-BSA for 12 h with vehicle (none; sample 1), 0.01 μM 9,13dcRA (sample 2) or the same concentration of Ch55 (sample 3), in the absence (open columns) and presence of 1 μM RARα-selective antagonist, Ro41-5253 (closed columns), or RARβ-selective antagonist, LE135 (slashed columns). Cellular PA activities (panel A) and active TGF-β levels in the medium (panel B) were measured as before. *: $P<0.01$.

activation of RARα as the first step. The result in Fig. IV-7 suggests that 30~40% of the induction by 9,13dcRA was independent upon RARα. It is reported that RARα is expressed in both quiescent and transformed HSCs *in vivo*, whereas RARβ expression is down-regulated during the transformation in the cultures and in the fibrotic liver (105). Taken together with the findings that both RARβ- and RARγ-selective retinoids failed to induce tPA and TGF-β in HSCs and that RARβ-selective antagonist did not significantly block 9,13dcRA-induced up-regulation, it is suggested that RARβ and RARγ seemed to have relatively less effects on tPA induction and subsequent TGF-β formation.

Enhancement of fibrogenic mediators by 9,13dcRA

It was very likely that induction of TGF-β activity by 9,13dcRA might result in the stimulation of collagen synthesis in HSC cultures. I next confirmed this point by measuring changes in collagen at both mRNA and protein levels following 9,13dcRA treatment of LI90 cells cultures for various periods of time (Fig. IV-8). As seen in *panel A*, proα_2 (I) collagen mRNA levels were significantly elevated after 9 h, and its protein levels biphasically increased, with the first peak occurring at 9 h and the later increase up to 72 h (*panel B, curve a*). These increases were significantly suppressed by the inclusion of a plasmin inhibitor, aprotinin (*curve b*) or α_2-antiplasmin (open square) as well as anti- TGF-β antibodies (*curve c*), indicating that induction by 9,13dcRA of collagen synthesis in HSC cultures is dependent upon plasmin generation of TGF-β. Similar results were obtained using the primary cultures of rat HSCs following treatment with atRA or 9,13dcRA (Fig. IV-9). Together with the above results, it is suggested that 9,13dcRA as well as atRA might be fibrogenic in the process of liver fibrosis.

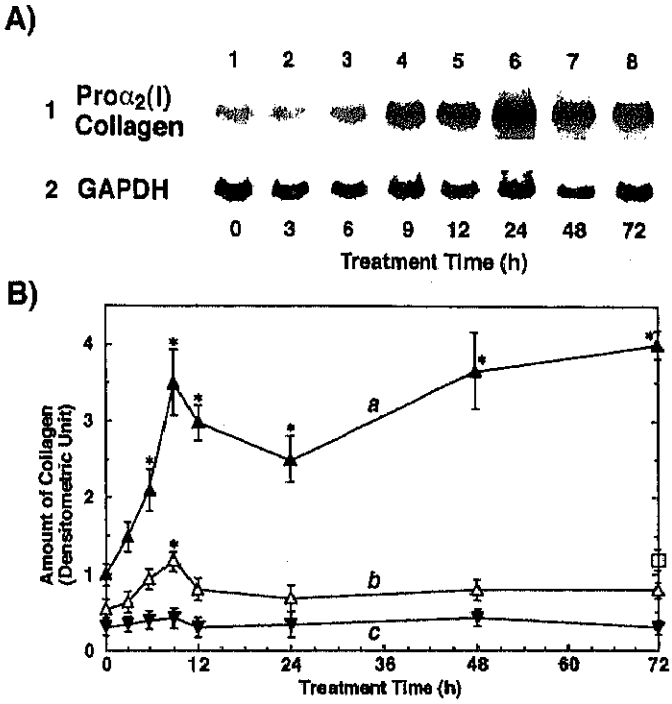

Fig. IV-8. Fibrogenic activity of 9,13dcRA in human HSC cell cultures. A) After confluent LI90 cell cultures were incubated with 1 μM 9,13dcRA in serum-free DMEM containing 0.2% bovine serum albumin for various lengths of time, cell lysates were prepared and total RNA was extracted. Each RNA (20 μg) was fractionated through 1% agarose-formaldehyde gels, transferred to nylon membranes, and hybridized with ^{32}P-labeled probes for proα_2(I) collagen and GAPDH. The radioactivity of each band was quantitated on an image analyzer. The experiment was repeated twice, and a representative result is shown. B) The cultures were treated with 1 μM 9,13dcRA for various lengths of time in the absence (curve a) or presence of either 50 μg/ml aprotinin (curve b), 5 μg/ml α_2-antiplasmin (open square) or 25 μg/ml anti-TGF-β antibody (curve c). At the indicated times, cultures were metabolically labeled with [^{3}H]proline and extracted with Triton X-100 and assayed for type I collagen as described in the Materials and Methods. Each value in curves a-c represents the average ± SD (n=3). Asterisks represent significances ($p<0.05$) obtained by a comparison to control (time 0) calculated by Dunnett's *t*-test. Each experiment was repeated three times and representative results are shown.

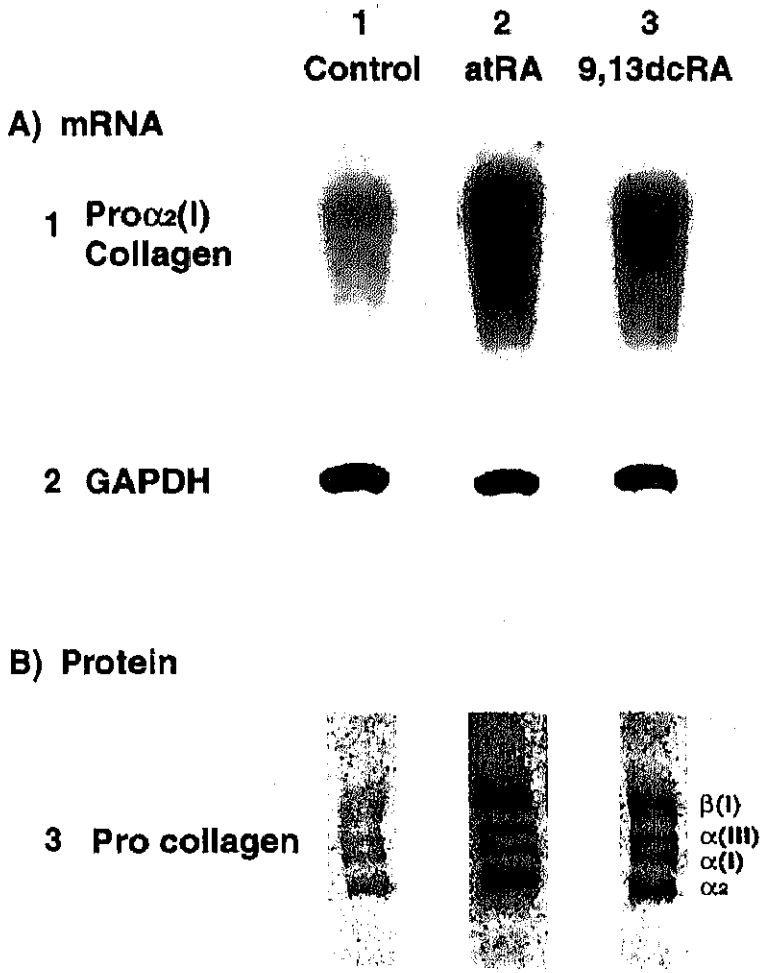

Fig. IV-9. Fibrogenic activity of 9,13dcRA in rat HSC cultures. A) After confluent rat HSC cultures were incubated with 1μM atRA or 9,13dcRA in serum free DMEM containing 0.2% bovine serum albumin for 24 h, cell lysates were prepared and total RNA was extracted. Northern analyses for proα_2 (I) collagen and GAPDH were performed as described in the legend to Fig. IV-8. B) The cultures were treated with 1 μM atRA or 9,13dcRA for 24 h and metabolically labeled with [^{3}H]proline as described in the legend to Fig. IV-8. Data are presented as the fluorogram of each sample. Positions of each of standard collagens are indicated in right margin. Each experiment was repeated three times and representative results are shown.

Table IV-1 is the summary of changes in hepatic mRNA expression of RARα/β, tPA, TGF-β, and collagen, fibrogenic mediators augmented in 9,13dcRA-treated HSC cultures. In fibrotic rats, hepatic levels of RAR, PA, TGF-β, and proα_2 (I) collagen mRNAs increased 40~100% compared to those in control rats. These results suggest that in porcine serum model of rat hepatic fibrosis, retinoid loss is correlated with increased formation of atRA as well as 9,13dcRA, and that similar changes, induced in HSC cultures with these compounds (Figs. IV-5 and IV-8), were evoked in the liver.

Acceleration of hepatic fibrosis in rat livers by exogenously added retinoid

Next, I examined whether exogenously added retinoid could exacerbate the fibrosis induced by porcine serum-treatment. Twelve weeks after starting the administration of porcine serum, a significant difference was observed in the degree of liver fibrosis between the porcine serum group that had been treated with porcine serum alone and the porcine serum plus retinoid group that had been treated with porcine serum plus stable RA analog. Histologic evaluation showed that almost all the rats treated with porcine serum alone had slight fibrosis (grade I; Fig. IV-10A) except for one with moderate fibrosis (grade II), whereas all the rats treated with porcine serum plus the retinoid had liver cirrhosis (grade III; Fig. IV-10B). In the porcine serum group (*panel A*), the connective tissue fibers and slight septal fibrosis appeared. In the porcine serum plus retinoid group (*panel B*), connective tissue septa linked portal tracts with central canals, separated and surrounded most of parenchymal fragments, generating pseudolobuli. The histologic grade of porcine serum plus retinoid group (3.0 ± 0.0, the average $\pm$ SD, n=10) was significantly ($p<0.05$) higher than that of porcine serum group (1.1 ± 0.3, n=10). In both groups the parenchyma appeared undamaged, and

Table IV-1. Comparison of mRNA levels of fibrogenesis-related genes between the control and porcine serum-administered rats.

mRNA	Control Rats	Fibrotic Rats	% change
RAR	96 (87-121)	134 (119-173)*	+40
PA	102 (78-120)	168 (114-183)*	+65
TGF-β	97 (92-114)	189 (167-207)*	+95
Collagen	123 (53-134)	246 (159-316)*	+100

* $p<0.05$ between control and fibrotic rats by Mann-Whitney-Wilcoxon test.

Six rats each were treated with either saline (control) or porcine serum for 12 weeks. Animals were sacrificed, livers were isolated, and total RNA was extracted from each liver. The relative levels of RARα/ß, tPA, TGF-β, and proα$_2$ (I) collagen mRNA were assessed by Northern blotting as described in the Materials and Methods, evaluated by densitometric analyses, and calculated as percentages of the average of each control after normalization against mRNA levels of GAPDH. Data are expressed by median with range in parenthesis.

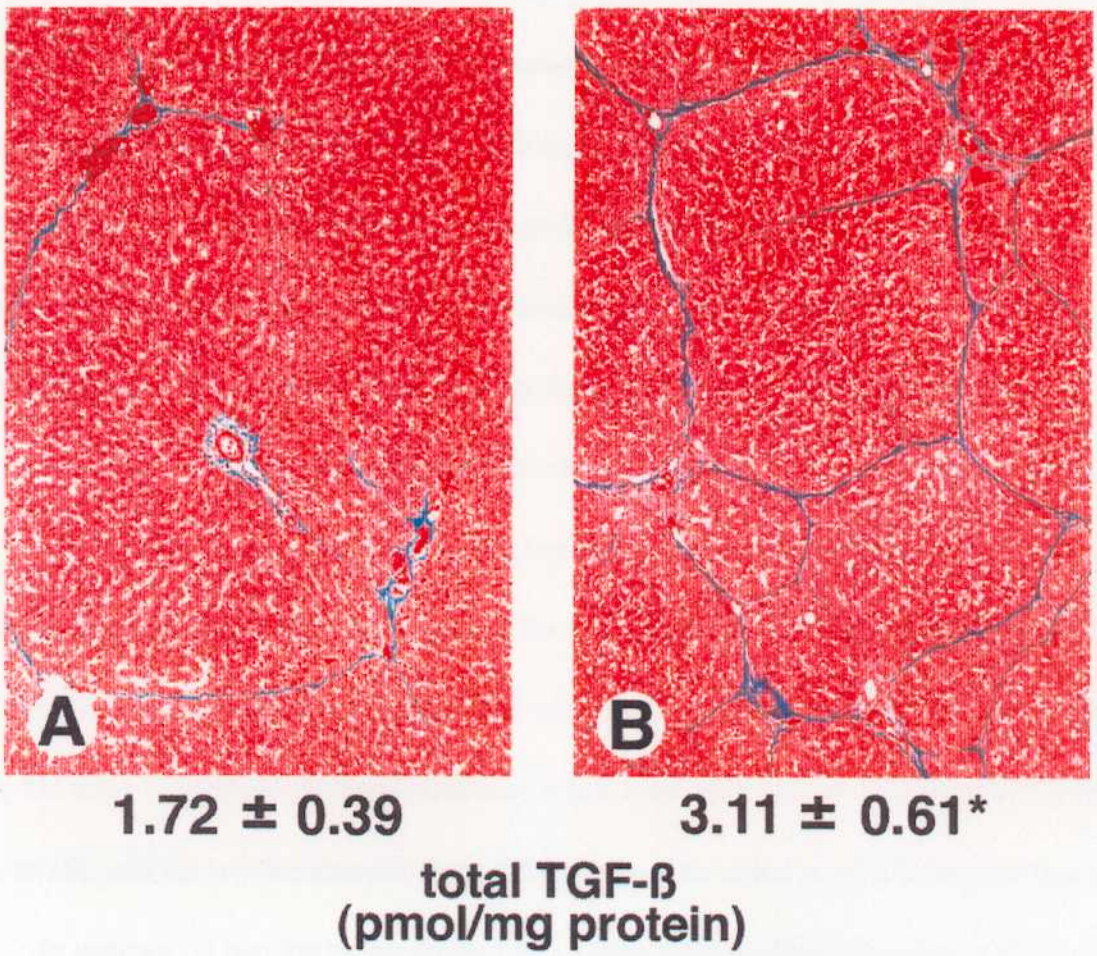

Fig. IV- 10. Acceleration of porcine serum-induced hepatic fibrosis in rat livers by a synthetic retinoid. Livers were harvested from Wistar rats 12 weeks after starting the administration of porcine serum without (panel A) or with (panel B) an acyclic retinoid. Half of the livers was fixed, sectioned, stained according to the method of Azan-Mallory, and evaluated histologically for fibrosis and cirrhosis. Magnification, x50. The total TGF-β levels in acid-ethanol extracts derived from another half of each liver were measured and expressed under the panel as pmol per mg of protein in the sample. Each value represents the average ± SD (n=10). An asterisk represents significant difference ($p<0.05$) between two groups. Representative results are shown from three separate experiments.

there was no evidence of fatty degeneration, necrosis, or regeneration. The administration of the retinoid alone to normal rats did not cause any apparent changes in the liver (n=10). Table IV-2 summarizes the result of hydroxyproline quantitation as an index of hepatic collagen contents. Comparing to the negative control (*lane 1*), hydroxyproline levels increased 4% and 38% following the treatment for 12 weeks with either the retinoid (*lane 2*) or porcine serum (*lane 3*), respectively. In contrast, a 158% increase was observed by simultaneous administration of the retinoid and porcine serum (*lane 4*). There was no obvious difference in the weight of livers among these four groups. The similar change was observed in the levels of proα2 (I) collagen mRNA expression in the liver (data not shown). At the same time, I measured hepatic TGF-β levels. Since I could not measure the amount of active TGF-β due to the technical issue that nonspecific activation of latent TGF-β occurred during the preparation of samples, I could only compare the total TGF-β levels in the liver. Normal rat livers contained a low level of total TGF-β (1.06 ± 0.23 pmol/mg protein, n=10), and the acyclic retinoid alone did not affect this value (1.15 ± 0.30 pmol/mg protein, n=10). In contrast, in porcine serum-treated rats, I detected a moderate increase ($p<0.05$) after the simultaneous retinoid-treatment as shown under the panels in Fig. IV-10. A similar enhancement was observed in TGF-β2, but not TGF-β1 and -β3 mRNA expression (data not shown).

Table IV-2. Potentiation by the synthetic retinoid of the enhancement of liver hydroxyproline levels in experimental rat models

Treatment		Hydroxyproline contents (μg/g liver)	
P.S.	Retinoid	8 weeks	12 weeks
-	-	178 ± 21 (n=5)	198 ± 36 (n=5)
-	+	190 ± 16 (n=5)	205 ± 30 (n=5)
+	-	241 ± 26 (n=5)	273 ± 14 (n=5)
+	+	290 ± 34 (n=5)	511 ± 125 (n=5)*

Wistar rats were treated with porcine serum (P.S.) and/or the synthetic retinoid (Retionid) for either 8 or 12 weeks. Livers were harvested, weighed, and assayed for hydroxyproline contents. Each value represents the average ± SD (n=5).

A representative result from three independent experiments is shown.

*$p<0.05$, obtained by a comparison with other seven groups.

IV-4. Discussion

It is well known that the retinol content of HSCs decreases along with the development of liver fibrosis (87). However, the detailed mechanism of the loss of retinol droplets, as well as the distribution of retinol and its metabolites remained unclear. Once RAs are formed, they cannot be either reduced back to retinol or stored as retinyl esters. Thus, the loss of retinyl esters observed in fibrotic liver might be, in part, the result of conversion to atRA and/or to further metabolites including 9cRA, 13cRA, and 9,13dcRA. In agreement with this hypothesis, I have documented, respectively, 58% and 114% increases in the generation of atRA and 9,13dcRA in fibrotic rat livers. Similar, however, smaller changes (about half of those observed *in vivo*) were observed during the activation of HSCs *in vitro*. Furthermore, in support of this proposed mechanism, hepatic levels of RAR, PA, TGF-β, and proα_2 (I) collagen mRNAs also increased by 40~100% in these same fibrotic rats. Because 9,13dcRA is a major product arising from the *in vivo* isomerization of 9cRA (93, 103, 104), the elevation in hepatic 9,13dcRA implies that retinoid metabolism would be stimulated, and that atRA and, subsequently, 9cRA might be generated during the development of fibrosis. Interestingly, I could not detect 9cRA in both activated HSCs and the fibrotic liver. I speculate that this discrepancy might imply a rapid isomerization of 9cRA in the activated HSCs and rat injured livers, or alternatively, a novel pathway of RA metabolism.

Collectively, the current findings suggest that during the development of liver fibrosis, endogenous RAs might be produced which stimulate PA/plasmin formation of TGF-β probably through physical interaction between RAR/RXR and Sp1, culminating in the augmented collagen synthesis, thus promoting fibrogenesis. However, much remains to be elucidated. First, it is important to establish the cell type producing atRA and/or 9,13dcRA *in vivo*. Although the

increases of atRA and 9,13dcRA were only 58% and 114%, respectively, if these RAs are elevated only in a single cell type, then measurement of whole liver levels actually dilutes the relative increase, and could be far more substantial if measured on a per cell basis. In fact, it is reported that hepatocytes and vascular endothelial cells exhibit differential metabolic and isomerization rates for atRA and 9cRA (104). However, it was technically difficult to isolate each liver cell type and extract sufficient retinoid from each cell without the possibility that RAs would be generated during the cell isolation procedure. Therefore, I examined whether RAs might be generated in HSCs during their *in vitro* activation by culturing them on plastic dish. Indeed, there were, respectively, 33%, 33%, and 60% increases in atRA, 13cRA, and 9,13dcRA, between 1 day cultures and 7 day cultures, suggesting that HSCs have ability to convert retinol to RAs during their activation process. It would be possible that RAs were generated in HSCs during the first day of their culture. However, again, this could be hardly proved as extraction of sufficient retinoid from isolated HSCs is difficult without increasing cell numbers by tissue culture. Although I showed that HSCs are likely to be responsible for RA generation, I can not exclude the possibility that retinol might be transferred from HSCs to surrounding hepatic cells and there converted to RAs *in vivo*.

Second, it is important to determine which RA isomer is more causally related to fibrogenesis. Although I proved that 9,13dcRA itself is fibrogenic *in vitro*, it is possible that increased atRA is more relevant, and the observed increase in 9,13dcRA merely reflects the increase of pre-existed atRA and 9cRA. In this case, provided that all of the 120 pmol/g tissue 9,13dcRA increased are the result of isomerization of atRA, it is estimated that 123 (3 + 120) pmol/g tissue atRA should be newly produced, out of which 95% (120 pmol/g tissue) is finally converted to 9,13dcRA. Third, it will be important to determine what percentage of retinol stored in HSCs is converted to 9,13dcRA.

Again, if the source of increased 9,13dcRA is solely retinol, based on our data, at least 2.7% of consumed retinol (4.4 nmol/g tissue) is assumed to be converted to 9,13dcRA (120 pmol/g tissue).

Finally, it is most important to clarify how porcine serum-treatment stimulates accumulation of 9,13dcRA, and whether a similar response occurs in other forms of liver fibrosis. Ohata et al. (107) reported that in bile duct ligation model of rat cholestatic liver fibrosis, hepatic RA levels were lowered by 60% and expression of RARß and RXRα was reduced by 17~20%, resulting in diminished retinoid signaling. Thus, retinoid metabolism and subsequent biologic changes may differ between different models of hepatic fibrosis. In fact, I have observed the conflicting effects of RA on liver fibrosis depending upon two different animal models either with or without hepatic parenchymal necrosis (108). In CCl_4-treated rats, in which liver fibrosis was accompanied by parenchymal damage, a stable analog of RA suppressed the progression of fibrosis indirectly by reducing hepatic necrosis, probably via in part interference with the secretion of tumor necrosis factor-α (TNF-α) from Kupffer cells (109). On the other hand, the same retinoid exacerbated liver fibrosis in porcine serum-treated rats, in which hepatic fibrosis was induced without parenchymal necrosis, via direct action of retinoid on HSCs; it enhanced PA/plasmin levels, activated latent TGF-β on the cell surface, and induced TGF-β -mediated production of collagen. Thus, apparent conflicting effects of RA on liver fibrosis may partly be explained by the difference in target genes and target cells on which RA affected under respective conditions. Davis and co-workers (110-112) have reported that interstitial collagen and/or TGF-β production is either increased, unchanged, or reduced by the exposure of rat HSCs to atRA or TGF-β, implying again that the difference(s) in the experimental conditions, especially the different stages in the transformation of HSCs used for the experiments, caused the opposing effects of RA on liver fibrosis.

The detailed mechanisms of these differences remain unclear.

In summary, the present study suggested that (1) there is a potential link between 9,13dcRA formation and hepatic fibrosis via formation of TGF-β *in vivo* porcine serum-induced liver fibrosis model, that (2) 9,13dcRA transactivates RARα, and provokes PA/plasmin and TGF-β-dependent procollagen synthesis in HSC cultures, and that (3) exogenously added retinoid accelerates the porcine serum-induced fibrosis by enhancing TGF-β contents and collagen levels in the liver.

IV-5. Summary

During hepatic fibrosis, HSCs transform into myofibroblastic cells and lose their intracellular droplets of retinyl esters, the storage form of vitamin A. An aim of this chapter is to address a potential link between the loss of retinyl esters to increased formation of RA(s), which might play a role in facilitating TGF-β-mediated liver fibrogenesis. The levels of 9,13dcRA, a novel and endogenous stereoisomer of atRA, were increased both in activated HSCs *in vitro* and in fibrotic liver. 9,13dcRA bound to and activate RARα, and provoked PA/plasmin, thereby, surface plasmin levels, and induced the activation of latent TGF-β in LI90 cells. Similar effects were obtained with RARα-selective retinoid, but not with RARβ- or RARγ-selective retinoid, and the induction was inhibited by RARα-selective antagonist. *In vivo* rat models, a RA analog accelerated the porcine serum-induced fibrosis by enhancing TGF-β contents and, thus, collagen levels in the liver, although the RA analog alone was not fibrogenic. These findings suggest a potential link between 9,13dcRA formation and hepatic fibrosis via formation of TGF-β *in vivo*, and thus provide further insight into the biologic role of retinoids during hepatic fibrogenesis.